PAPER • **OPEN ACCESS**

The vacuum chamber for the APPLE-X undulators at the European XFEL

To cite this article: D. La Civita *et al* 2022 *J. Phys.: Conf. Ser.* **2380** 012020

The vacuum chamber for the APPLE-X undulators at the European XFEL

D. La Civita[1], S. Casalbuoni[1], S. Karabekyan[1], M. Planas[1], H. Sinn[1], T. Wohlenberg[2], M. Wünschel[1], F. Yang[1]

[1] European XFEL GmbH, 22869 Schenefeld, Germany
[2] Deutsches Elektronen-Synchrotron, 22607 Hamburg, Germany

Mail: daniele.lacivita@xfel.eu

Abstract. Thanks to the installation of four APPLE X helical undulators, the SASE3 soft X-ray beamline at European XFEL will provide to the experimental stations the polarization control of the X-rays. The helical undulators are located downstream with respect to the already existing planar undulators. The design of the magnetic active parts and of the helical undulator support structure requires a new design of the vacuum chamber and its alignment system. This contribution describes the mechanical design, production process, UHV qualification process and alignment of the vacuum chamber.

1. Introduction

At European XFEL three beamlines are currently in operation, two hard x-ray beamlines, SASE1 and SASE2, that cover the photon energy range from 3.6 to 25 keV and one soft X-ray beamline, SASE3, that operates in the photon energy range from 500 to 3000 eV [1, 2]. All the beamlines generate linearly polarized radiation in the horizontal plane. In the soft X-ray beamline, in order to provide variable polarization and therefore extend the set of possible experiments, four new APPLE X helical undulators have been recently installed and are now in the phase of commissioning with the electron beam. The new undulators with 90 mm period length are installed after the 21 already existing and fully commissioned, planar undulators with 68 mm period length and can provide different polarization modes: right and left circular, elliptical and linear polarization at an arbitrary angle [3].

The APPLE X undulators were developed by the Paul Scherrer Institute (PSI) in Switzerland for the FEL beamlines of SwissFEL [4-6]. A collaboration agreement between PSI and European XFEL was set and the scope of the agreement was the delivery of the undulator mechanical structures and the finalization of the magnetic design in collaboration with European XFEL. The vacuum chamber, due to different interfaces and requirements between European XFEL and PSI was not included in the agreement and had to be designed by European XFEL in close collaboration with DESY vacuum group.

2. Requirements and design

The undulator frame design and the remotely controlled undulator alignment system pose relevant boundary conditions for the design. To improve the undulator frame stability and minimize the frame deformation under the high and variable in direction magnetic forces, the frame has a closed O shape. Therefore the chamber, along the undulator, cannot be supported from the floor. Moreover, the undulator sits on movers based on rotating eccentric systems (cams) for the precise beam-based alignment and the undulator alignment range should be taken into account when the chamber dimensions are defined.

Figure 1 shows the APPLE X structure with the magnetic structure mounted on the cam movers. To cope with both constraints, we decided to support the chamber from the frame, in this way the chamber follows the movement required for the alignment of the undulator. We supported the chamber on two points in order to avoid an hyperstatic mounting that, even if provides more controls points, can generate a hardly predictable deformed shape.

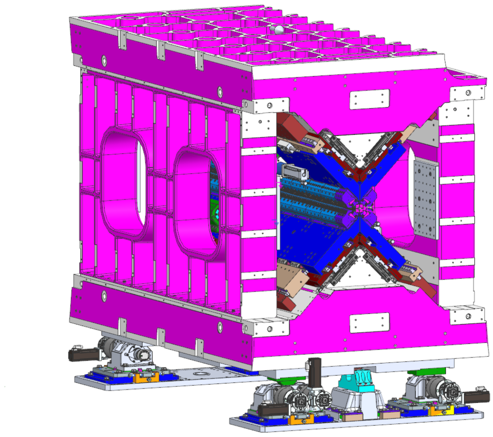

Figure 1. Downstream view of the APPLE X structure. In violet the frame, in blue the movable arrays and in light blue and purple the magnetic structure with magnetic terminations. Vacuum chamber and alignment quadrupoles have been hidden. Cam movers are visible on the bottom of the structure.

The supporting points allow also the alignment of the chamber and one of them is a fixed point in longitudinal direction while the second, downstream, implements a flexure to cope with the chamber thermal deformation. The alignment range and resolution in both horizontal and vertical direction are ±1.5 mm and 10 μm respectively. The rotation of the chamber around its axis can also be corrected and the requirements for this degree of freedom are ±5° range and 0.05° resolution.

The electron beam stay clear aperture is 8 mm in diameter while the undulator stay clear aperture, the nominal minimum gap, has a diameter of 12 mm. The total length, flange to flange of the chamber is 2394 mm and the length of the undulator magnetic structure is 1980 mm and can move longitudinally ±45 mm. Starting from the electron and undulator stay clear apertures and taking into account alignment range of the undulator (± 0.2 mm), mechanical straightness of the extruded chamber (± 0.25 mm), sag due to gravity (0.3 mm) and some final clearance between chamber and magnets (0.1 mm) we derived the dimensions of the chamber core: inner and outer diameter are 9.4 mm and 11 mm respectively, the thickness of the chamber wall is therefore 0.8 mm.

The material chosen for the chamber is EN AW-6060T6 (AlMgSiT6). Being an Aluminum alloy, the material presents very low magnetic permeability, as required by the accelerator specifications, but is also very suitable for extrusion and can be welded to allow the assembling of the machined extrusion with the bimetal CF flanges.

To increase as much as possible the area moment of inertia of the cross section taking into account extrusion constraints that limit the total cross section dimensions, verticals and horizontal fins were implemented giving to the extrusion the shape like a cross.

The vacuum chamber needed also to be water cooled to keep the temperature of the permanent magnet stable and had also to provide the possibility to wind, along the entire length, horizontal and vertical corrections coils for the compensation of the ambient magnetic field. For those purposes, along the stiffening fins, the chamber cross section had to implement also expansions to host the holes. Figure 2 shows the chamber cross section with the main dimensions. Along the central hole travel the electrons and the two holes above and below the beam vacuum core are for the horizontal correction coil while in the horizontal plane the 5 mm diameter hole are for the cooling system and the 6 mm diameter ones are for the vertical correction coil. The grooves on the extremities of the horizontal fins are designed to provide a holding interface for light radiation and temperature sensors. Figure 3 shows the chambers and the magnetic arrays in minimum (figure 3a) and maximum (figure 3b) magnetic gap configuration.

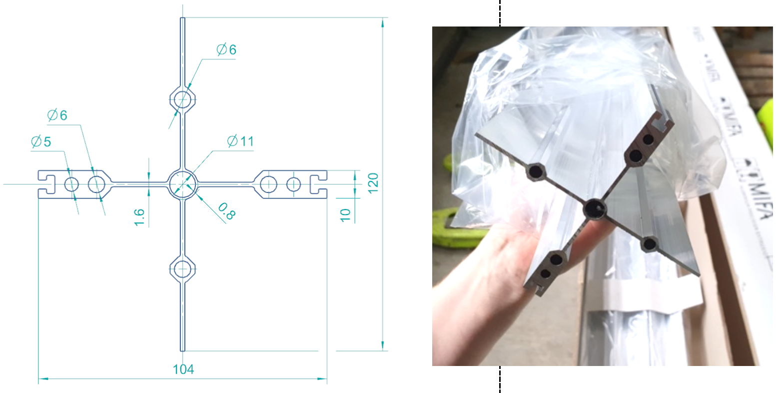

Figure 2. Picture and Cross section of the extruded profile with main dimensions.

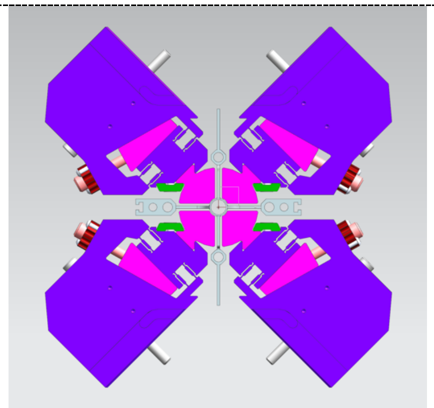

Figure 3a. Chamber and magnetic arrays at minimum gap.

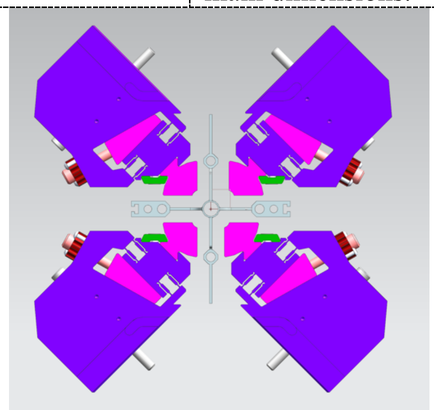

Figure 3b. Chamber and magnetic arrays at maximum gap.

The thermal load that has to be dissipated by the cooling system consists of the heat produced by Joule effect on the compensation coils (16 W for the vertical correction coil and 0.6 W for the horizontal correction coil) and the heat generated by the synchrotron radiation and the dissipation of the wakefield (10 W). Steady state thermal simulation in Ansys show that the maximum ΔT is below 0.5 K that is compliant to the initial requirement. In the simulation any radiative cooling in air is neglected and on the surface of the water channels a film coefficient of 5800 W/m^2K is applied.

Static structural analyses were performed to verify the thickness of the vacuum chamber wall against the atmospheric pressure and the walls of the water channels against the pressure of the water distribution system (7 bar). The maximum von-Mises stress is about 1.5 MPa, therefore well within the max yield strength of the material.

The sag due to gravity was also evaluated by FE analysis and it results in less than 300 μm. Figure 4 shows the magnified vertical deformation. The mass of the water in the cooling channels and of the copper wire for the compensation coils was also taken into account because it represents a not negligible contribution to the total mass, the chamber is very light, only 3.8 kg for 2.4 m long profile.

Due to the ratio between length and cross section and the axial load that can be produced by the flexure that connects the chamber to the alignment stage we performed also analytical and numerical buckling analyses. With perfect alignment, analyses show that the first buckling modes can happen at axial loads more than 30 times higher than the maximum expected axial load. According to the numerical simulation results, about 2 mm compression in the longitudinal direction will induce buckling failure of the structure. The misalignment in the other two directions is less critical. Buckling due to geometrical imperfections was not taken into account due to the high safety margin shown in the previous instability analyses. Figure 5 shows the result of the first two bucking models of the chamber under axial load.

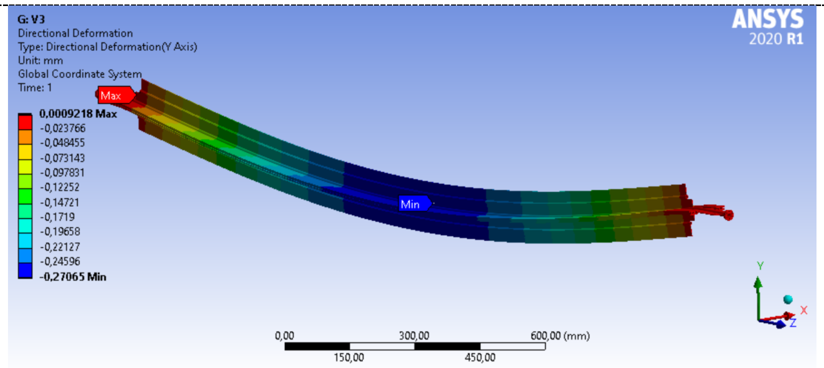

Figure 4. Deformation in mm due to gravity force applied on chamber body, correction coils wires and cooling water.

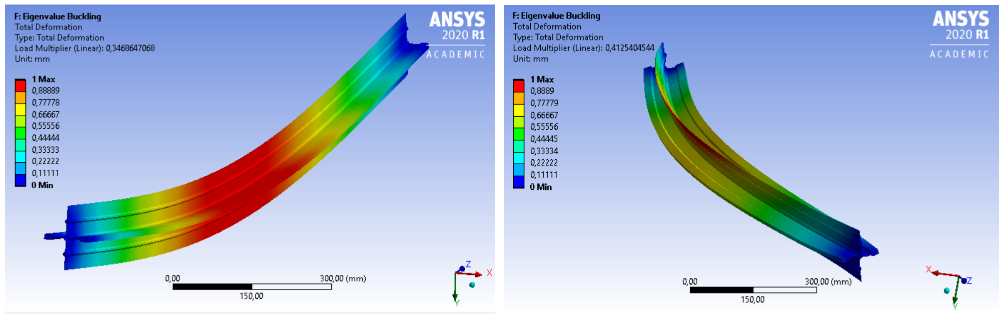

Figure 5. First (left) and second bucking mode with perfect geometry under axial load.

Nonlinear numerical analyses were also used to validate the residual stress and von-Mises stress in the area of the welding of the flange with the chamber and to design properly the geometry of the flexible element that allows the thermal expansion and contraction of the chamber. The flexure is made of Titanium alloy (Ti6Al4V) due to its good mechanical and magnetic properties (yield strength about 1.1 GPa and low magnetic permeability) and can cope with an axial movement of ±0.6 mm and produce a maximum reaction force of 40 N.

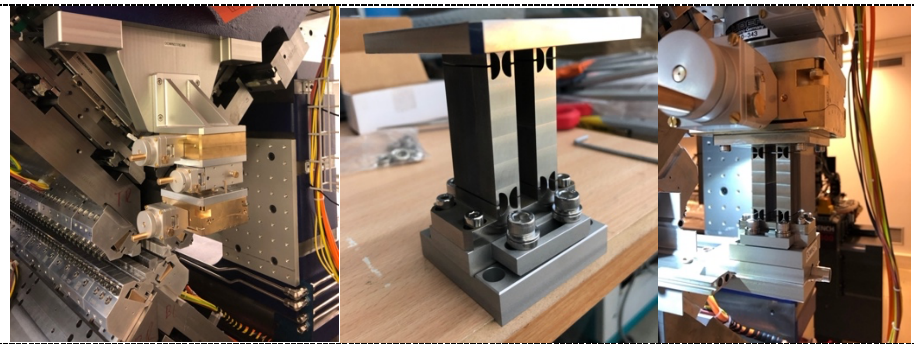

Figure 6. From left to right: stack of the 3 alignment stages; flexure assembly; chamber holding system.

The alignment system is mounted on the undulator frame and holds the chamber with clamps that are connected to the horizontal fins, in this way there is no compressive load on the vacuum pipe in the center of the chamber. The alignment system consists of a stack of 3 stages, one for each degree of freedom: vertical and horizontal translation and rotation around the chamber axis (see Figure 6).

The accelerator requirement of relative magnetic permeability < 1.01 for all elements within 300 mm from the electron beam poses clear challenges in the choice of the compliant stages. The company HUBER Diffraktionstechnik GmbH & Co. was able to provide manual stages with in-house measured, maximum relative magnet permeability of 1.005. The selected stages are 5101.80, 5103.A10 and

5202.60 for the horizontal, vertical and rotational degree of freedom respectively. Detailed specifications of the stages are available in [7].

3. Extrusion, manufacturing, welding and UHV conditioning and testing

The company MIFA Aluminium BV provided the 2.8m long, high-quality extruded profiles [8]. MIFA was interested in being involved in this project with a small, respect to industrial production, number of extruded profiles and provided important feedback about feasibility during the design phase. The extruded profiles were compliant to the tight mechanical tolerances of the cross section and the straightness and twist of the profile were better than 0.15 mm/m and 0.20 mm/m respectively. The direction of the concavity was indicated on the profile in order to mount the chamber with the concavity facing down and therefore compensating the gravitational sag.

The extruded profiles were chemically etched on the inner surface of the vacuum pipe by HENKEL Beiz- und Elektropoliertechnik GmbH & Co [9]. The procedure was aimed to smooth the roughness of the inner wall of the vacuum chamber. The treatment foresees the following steps: chemical/mechanical precleaning, rinsing with low conductance clean water, pickling of the internal surfaces with NaOH at 50-60°C, rinsing with low conductance clean water, internal passivation, final rinsing with low conductivity water, rinsing with deionized water and drying with Nitrogen. After the treatment, samples of the inner surface of one chamber were analysed with confocal laser scanning microscope and the roughness (Ra) was everywhere better than 0.3 μm and in some samples even below 0.1 μm.

The profile was machined by Witte Barskamp GmbH & Co [10]. Mechanical interfaces for the clamping system and preparation of the chamber extremities for the flange welding were machined out. Special supports for the clamping of the long chambers during machining were also developed.

The bimetal (Al/SS) CF10 flanges were laser welded by Hoedtke GmbH & Co [11]. Figure 7 shows a welding test and the detail of the section. The test samples were used to optimize the welding parameters and were leak searched to qualify the process.

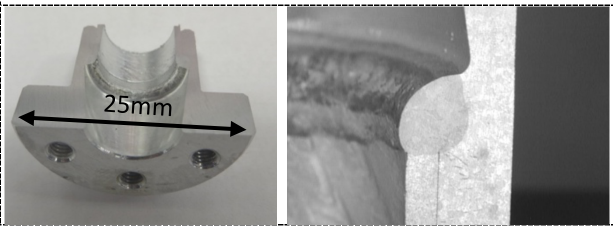

Figure 7. Laser welding test samples. In the right picture the welding seam is visible, it connects the flange pipe (external element) with the 0.8 mm thickness wall chamber (inner element).

The final UHV conditioning was carried out at DESY by the vacuum group (MVS). A special cleaning process was developed for the XFEL planar undulator chambers. This process was also adopted to the vacuum chambers for the APPLE-X undulators. The inner oxide layer was reduced below 5 nm and a special passivation treatment was carried out to avoid the regrown of the Al oxide layer. Each chamber was leak searched and underwent the RGA test (Figure 8).

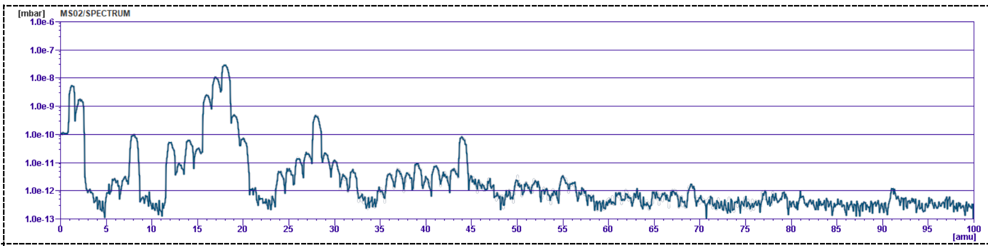

Figure 8. RGA spectrum of the APPLE-X vacuum chamber #2.

4. Alignment

The chamber was installed sliding it with the help of plastic shims along the magnetic arrays at the maximum possible gap. The chamber was clamped in the holding system and mechanically connected to the alignment stages. The alignment was performed with the help of pre-calibrated Micro-Epsilon capacitive sensors [12]. Flat capacitive sensors mounted on a 148 mm long, 1 mm thick plastic plate, were inserted between the magnets and fins of the chamber. Figure 9 shows the measurement system arrangement. We used eight capacitive sensors, two for each quadrant. A steel foil is attached to the side of the sensor facing the vacuum chamber. The contact between the sensor and the magnet is guaranteed by the magnetic force, therefore the reading of the sensor can be considered the absolute distance between magnet and chamber. The sensors model is CSG1.00-CA and has 2 mm measuring range and nominal static resolution of 8 nm.

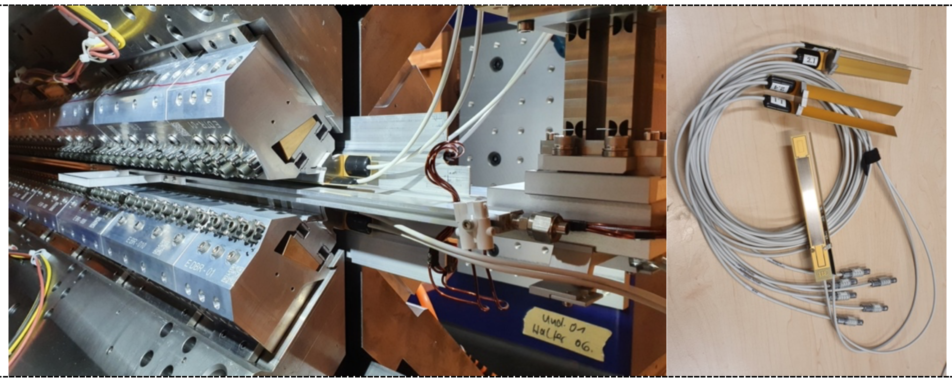

Figure 9. The capacitive sensors and on the left, their arrangement for the chamber alignment.

The alignment of the chamber was performed sequentially on each side of the chamber. Looking simultaneously at the sensor reading and moving the manual stages sequentially we tried to minimize the difference between the readings of facing sensors. We considered the alignment achieved when that difference was below 100 μm for all sensor pairs.

The central part of the chamber is not easily visually and mechanically accessible and to verify that there wasn't any contact between the vacuum chamber and the magnets, a final test has been performed. The undulator gap was set to its minimum (diameter of 12.5 mm) and a 60 μm thick, Kapton foil was passed along the entire length of the gap between the vacuum chamber and each quadrant of the magnetic structure.

References

[1] W. Decking et al., 2020, A MHz-repetition-rate hard X-ray free electron laser driven by a superconducting linear accelerator, Nature Photonics, 14:6 391.
[2] S. Abeghyan et al., 2019, First operation of the SASE1 undulator system of the European X-ray Free-Electron Laser, J. Synchrotron Radiat.26, 302.
[3] S. Karabekyan et al., 2021, SASE3 variable polarization project at the European XFEL, Proc. of IPAC 21, TUPAB122.
[4] R. Abela et al., 2019, The SwissFEL soft X-ray free-electron laser beamline: Athos, Journal of Synchrotron Radiation 26(4): 1073-1084.
[5] T. Schmidt, M. Calvi, 2018, APPLE X undulator for the SwissFEL soft X-ray beamline Athos, Synchrotron Radiat. News, 31 (3), pp. 35-40
[6] X. Liang, M. Calvi, C. Kittel, N. Sammut, T. Schmidt, Advanced operational models of the apple x undulator, Proc. of FEL 19, pp. 541-544
[7] https://www.xhuber.com/en/
[8] https://mifa.eu/en
[9] https://henkel-epol.com/en
[10] https://www.witte-barskamp.com
[11] https://hoedtke.de
[12] https://www.micro-epsilon.com